



1 **Excitation of Delocalized Long-Lived States in Aliphatic Protons**
2 **at Low and High Magnetic Fields**

3

4 Sebastiaan Van Dyck, Coline Wiame, Kirill F. Sheberstov* and Geoffrey Bodenhausen

5

6

7 Chimie Physique et Chimie du Vivant (CPCV, UMR 8228), Département de Chimie,

8 École Normale Supérieure, PSL University, Sorbonne Université,

9

75005 Paris, France

10

11

12 *Corresponding Author:

13 Dr Kirill Sheberstov email: kirill.sheberstov@ens.psl.eu

14

15 To be submitted to Magn. Reson. (Groupement Ampere)

16

17 *SVD's ORCID: 0009-0005-7622-5753*

18 *KS's ORCID: 0000-0002-3520-6258*

19 *GB's ORCID: 0000-0001-8633-6098*

20

CW ORCID: 0009-0008-3517-3354

21



22

Abstract

23 Long-lived states (LLS) can be excited in geminal protons of aliphatic chains by mono- or
24 poly-chromatic spin-lock induced crossings (SLIC), i.e., by application of one or more
25 selective radio-frequency (RF) fields to create delocalised population imbalances between
26 states belonging to different symmetry under spin permutations. At low fields (in this work at
27 1.4 T, or 60 MHz for proton NMR), these experiments are challenging due to the proximity of
28 the chemical shifts and the need to consider the full untruncated J -coupling Hamiltonian. Five
29 molecules were studied in this work: ethanolamine, lysine, vitamin B1, metronidazole, and
30 phenoxyethylamine (POEA). For POEA and metronidazole, the LLS are reported for the first
31 time. Measurements were carried out at low and high magnetic fields (1.4 T and 11.7 T, or 60
32 and 500 MHz for protons) using 60 MHz Magritek and 500 MHz Bruker NEO spectrometers.
33 The rates $R_{LLS} = 1/T_{LLS}$ and $R_1 = 1/T_1$ were determined using monochromatic SLIC excitation
34 at both fields. We describe strategies for optimising SLIC conditions in cases where the signals
35 of neighbouring CH_2 groups are relatively close to each other.

36

37

Key words

38 Long-lived states; Field-dependent relaxation; Spin-lock induced crossings.

39



40

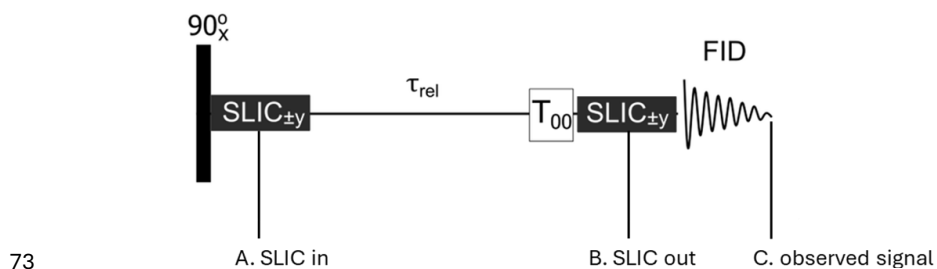
Introduction

41 A long-lived state (LLS) is a nuclear spin state that has a lifetime longer than the longitudinal
42 relaxation time [Carravetta et al., 2004]. Usually, an LLS corresponds to an imbalance between
43 states with different spin permutation symmetries [Stevanato et al., 2015, Sheberstov et al.,
44 2019a, Sabba et al. 2022]. In an isolated two-spin system with two protons H_A and $H_{A'}$, such
45 an imbalance can occur between the average population of three symmetric triplet states ($|T_1\rangle$,
46 $|T_0\rangle$, $|T_{-1}\rangle$) and the population of the singlet state ($|S_0\rangle$), which is antisymmetric under spin
47 permutation. The resulting population imbalance is immune to relaxation due to the dipole-
48 dipole coupling between the two protons H_A and $H_{A'}$, thus resulting in a long-lived state. In
49 short *achiral* aliphatic chains $-(CH_2-CH_2)-$ with 4 protons, the geminal proton pairs are
50 chemically equivalent because of the lack of stereogenic centers, but they can be magnetically
51 inequivalent provided each CH_2 group has a distinct chemical shift and provided the vicinal
52 scalar couplings between neighbouring CH_2 groups differ. This occurs if the populations of the
53 rotamers that result from rotations about the C-C bond are *not* equal, so that the differences
54 between the vicinal couplings $\Delta J = J_{AX} - J_{AX'} = J_{A'X} - J_{A'X'}$ do not vanish. Magnetic
55 inequivalence allows one to excite an LLS that is *delocalized* across the two AA' and XX' spin
56 pairs. This can be achieved by mono- or poly-chromatic spin-lock induced crossings (SLIC)
57 [DeVience et al., 2013, Sonnefeld et al., 2022a, Sonnefeld et al., 2022b], i.e., by application of
58 one or two selective radio-frequency (RF) fields simultaneously. This paper focuses on mono-
59 chromatic SLIC excitation solely. At high fields (e.g. 500 MHz), the RF amplitude for single
60 quantum (SQ) conditions, must be $\nu_{SLIC}^{SQ} = 2J_{intra}$, where J_{intra} is an averaged value of the
61 intrapair coupling between the geminal protons, e.g. $J_{intra} = \frac{1}{2}\{^2J(H_A, H_{A'}) + ^2J(H_X, H_{X'})\}$.
62 A pulse duration $\tau_{SLIC}^{SQ} = 1/(|\sqrt{2}\Delta J|)$ suffices for SQ level-anti-crossing (LAC). After a variable
63 relaxation delay τ_{rel} , one applies a T_{00} filter which removes all terms other than the desired
64 population imbalance [Tayler et al., 2020]. A second SLIC pulse then reconverts the LLS into
65 observable magnetisation (Fig. 1).

66 Achiral aliphatic chains with suitable 4-spin systems are found in ethanolamine, lysine, vitamin
67 B1, metronidazole, and phenoxyethylamine (POEA) (Fig. 2). At high field (e.g., at 11.7 T or
68 500 MHz for protons), all aliphatic chains in Fig. 2 can be described as $AA'XX'$ systems in
69 Pople's notation. On the other hand, at low field (e.g., at 1.4 T or 60 MHz) these systems must
70 be described by $AA'BB'$ to account for the second-order couplings. We show that LLS in these

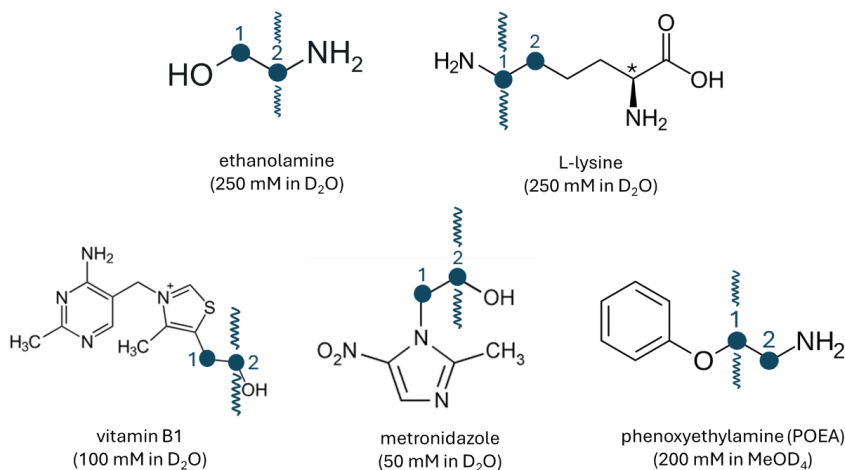


71 molecules can be excited efficiently at 1.4 T, despite the strong coupling regime, using re-
72 optimized SLIC sequences.



74 Figure 1. Sequence for the measurement of the relaxation times T_{LLS} of long-lived states (LLS) of protons in aliphatic chains
75 comprising AA'XX' or AA'BB' systems. The $\pi/2$ pulse brings the magnetisation into the transverse plane. The first Spin-Lock
76 Induced Crossing (SLIC) pulse converts this magnetisation into an LLS. This pulse is followed by a variable delay and a T_{00}
77 filter that retains only singlet order, while the second SLIC pulse reconverts the LLS into observable magnetisation. Cycling
78 of the RF phases along the $\pm y$ axes eliminates undesirable signals [Kiriyutin et al., 2016]. In AA'XX' or AA'BB' systems, the
79 SLIC pulses must be applied on resonance with either AA' or XX' spins.

80



81

82 Figure 2. Six molecules where long-lived states have been excited efficiently at both low and high static fields of 1.4 and 11.7
83 T (60 and 500 MHz for protons). All molecules shown are achiral and feature chemically equivalent but *magnetically*
84 *inequivalent* proton pairs AA'XX' at high field and AA'BB' at low field. The wavy arrows indicate the CH₂ groups that were
85 irradiated, in these experiments, to excite the LLS by mono-chromatic SLIC (arrows above the molecules), and to reconvert
86 the LLS into magnetisation (arrows below the molecules). Note that one can also reconvert LLS on the adjacent CH₂ group.
87 The relaxation rates $R_1 = 1/T_1$ of the CH₂ groups were also determined by the conventional inversion-recovery method. All
88 ligands were dissolved in D₂O at concentrations in the range between 50 and 250 mM, except for POEA which was dissolved
89 in MeOD₄.

90

91

92

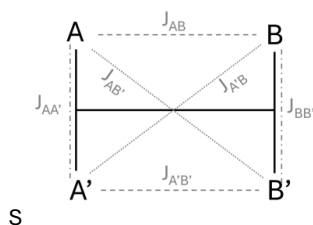


93

Methods

94 Strong Coupling at low field

95 As previously reported [Sonnefeld et al., 2022a, Sonnefeld et al., 2022b], the Hamiltonian of a
 96 4-spin AA'XX' system at high magnetic fields (in this work at 11.7 T) only features strong
 97 couplings between the geminal pairs (e.g., H_A couples strongly to $H_{A'}$), but not between the
 98 vicinal protons (since H_A couples weakly to H_X). At low field however, the vicinal couplings
 99 are also strong. The Hamiltonian can be represented by a topological diagram (Fig. 3) where
 100 the geminal J couplings $J_{AA'}$ and $J_{BB'}$ are approximately equal, while the vicinal couplings are
 101 pairwise degenerate $J_{AB} = J_{A'B'}$ and $J_{A'B} = J_{AB'}$.



102

Figure 3. Topological representation of a 4 spin AA'BB' system

104 The Hamiltonian in units of Hz is:

$$\begin{aligned}
 105 \quad H = & \nu_{AA'}(\hat{I}_{Az} + \hat{I}_{A'z}) + \nu_{BB'}(\hat{I}_{Bz} + \hat{I}_{B'z}) + J_{AA'}\hat{I}_A \cdot \hat{I}_{A'} + J_{BB'}\hat{I}_B \cdot \hat{I}_{B'} \\
 & + J_{AB}\hat{I}_A \cdot \hat{I}_B + J_{AB'}\hat{I}_A \cdot \hat{I}_{B'} + J_{A'B}\hat{I}_{A'} \cdot \hat{I}_B + J_{A'B'}\hat{I}_{A'} \cdot \hat{I}_{B'}
 \end{aligned}
 \tag{1}$$

107 Where \hat{I}_i corresponds to vector representation of spin operator of spin i , operators \hat{I}_{iz} represent
 108 z component of the operator \hat{I}_i . When switching from strong coupling at low field to weak
 109 coupling at high field, the non-secular terms of the vicinal J couplings (but not those due to the
 110 geminal couplings) can be dropped:

$$\begin{aligned}
 111 \quad H_{vic}^{LF} = & J_{AB}\hat{I}_A \cdot \hat{I}_B + J_{AB'}\hat{I}_A \cdot \hat{I}_{B'} + J_{A'B}\hat{I}_{A'} \cdot \hat{I}_B + J_{A'B'}\hat{I}_{A'} \cdot \hat{I}_{B'} \\
 & H_{vic}^{HF} = J_{AB}\hat{I}_{Az}\hat{I}_{Bz} + J_{AB'}\hat{I}_{Az}\hat{I}_{Bz'} + J_{A'B}\hat{I}_{A'z}\hat{I}_{Bz} + J_{A'B'}\hat{I}_{A'z}\hat{I}_{Bz'}
 \end{aligned}
 \tag{2}$$

113

114

115



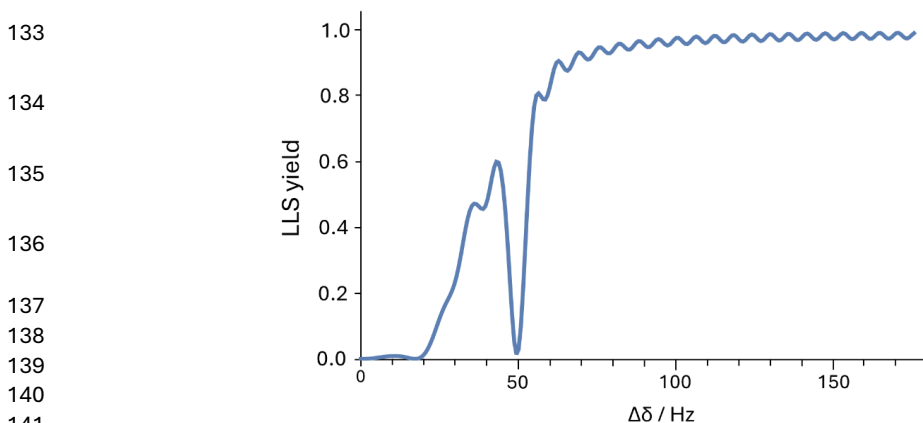
116 **Effects of second-order vicinal couplings**

117 In a low static field, a weak RF field applied to H_A and $H_{A'}$ also affects the protons H_B and $H_{B'}$
 118 by a Bloch-Siegert shift that modifies the effective resonance frequency of the non-irradiated
 119 spins. However, this does not have any dramatic consequences for mono-chromatic SLIC. At
 120 high field, these effects are negligible, so that monochromatic SLIC is truly selective. At low
 121 magnetic fields, we have investigated the effects of second-order couplings, for mono-
 122 chromatic SLIC excitation, using simulations with Spin Dynamica [Bengs et al., 2018] written
 123 using the Wolfram Mathematica software package.

124 In a 4-spin system $AA'BB'$, the LLS part of the density operator $\hat{\sigma}_{LLS}$, i.e., the population
 125 imbalances, always comprises three terms, regardless of how one excites the LLS [Sonnefeld
 126 et al., 2022a]:

127
$$\hat{\sigma}_{LLS} = \lambda_{LLS} \left(-\frac{1}{3} \hat{I}_A \cdot \hat{I}_{A'} - \frac{1}{3} \hat{I}_B \cdot \hat{I}_{B'} + \frac{8}{9} (\hat{I}_A \cdot \hat{I}_{A'}) (\hat{I}_B \cdot \hat{I}_{B'}) \right). \quad (3)$$

128 The LLS yields have been simulated for mono-chromatic SLIC irradiation applied to AA' . We
 129 chose typical values for a 4-spin system: $J_{AA'} = J_{BB'} = -14$ Hz, $J_{AB} = J_{A'B'} = 5$ Hz and $J_{A'B} = J_{AB'}$
 130 $= 9$ Hz, hence $\Delta J = -4$ Hz. At high fields, where the secular approximation can be invoked, the
 131 optimum RF amplitude for the single-quantum (SQ-LAC) condition is $v_{SLIC} = 2J_{intra} = -28$ Hz,
 132 and the optimum SLIC duration is $\tau_{SLIC} = 1/(\Delta J\sqrt{2}) = 177$ ms [Sonnefeld et al., 2022b].



142 Figure 4. Simulated yields of the excitation of a long-lived state (LLS) as defined in Eq. (3) as a function of the chemical
 143 shift difference ($\Delta\delta$) between the AA' and BB' spin pairs in a 4-spin system. Parameters of SLIC pulse were $v_{SLIC} = 28$ Hz
 144 and $\tau_{SLIC} = 177$ ms corresponding to the high-field SLIC conditions.

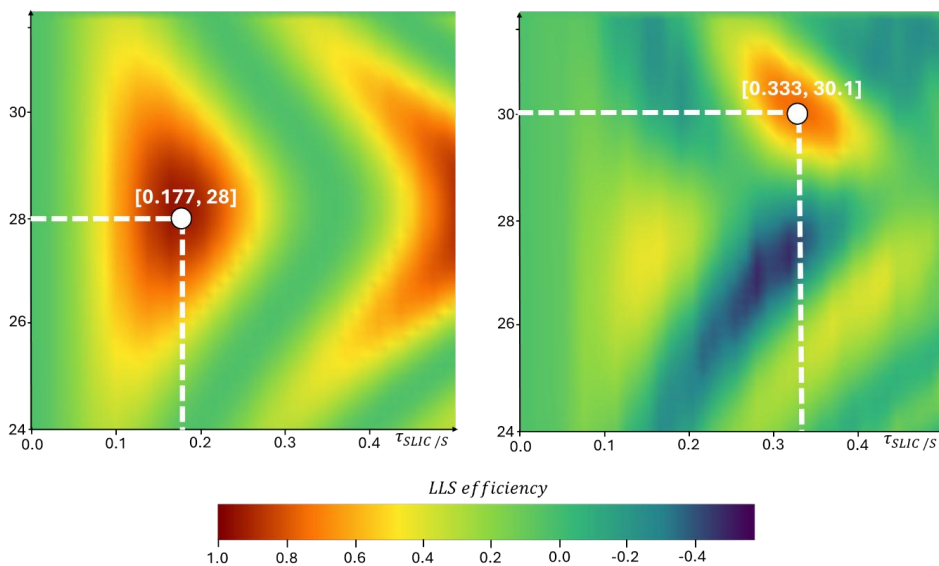
145

146



147 Fig. 4 also shows how the LLS yield depends on the chemical shift difference between spins A
148 and X denoted as $\Delta\delta$. The simulations were done for the case of high-field SLIC conditions (v_{SLIC}
149 $= 28$ Hz, $\tau_{\text{SLIC}} = 177$ ms). At $\Delta\delta > 60$ Hz the LLS yield reaches a plateau that we normalized to
150 1. The sudden drop in LLS yield, here at 50 Hz, depends on J_{intra} ; for higher values of J_{intra} ,
151 the dip shifts to higher frequencies. This means there is a “blind spot” where excitation of LLS
152 cannot be achieved, at least not starting with high-field SLIC parameters. In Fig. 4, under high-
153 field SLIC conditions ($v_{\text{SLIC}} = 28$ Hz, $\tau_{\text{SLIC}} = 177$ ms), the LLS yield is 1.0 for 250 Hz and
154 drops down to 0.35 for $\Delta\delta = 52$ Hz. Fig. 4 also shows how the LLS yield depends on the
155 chemical shift difference.

156 The simulations of Fig. 5 show how to optimize the RF amplitude v_{SLIC} and the SLIC duration
157 τ_{SLIC} , for the strong coupling regime and single quantum conditions, to achieve the best LLS
158 yields at different values for $\Delta\delta = 250$ Hz (high-field regime) and $\Delta\delta = 52$ Hz (low-field
159 regime).



160

161 Figure 5. Left panel shows that for a large difference $\Delta\delta = 250$ Hz, the single-quantum SLIC condition (RF amplitude v_{SLIC}
162 in the vertical dimension and the duration τ_{SLIC} in the horizontal dimension) for a 4-spin system ($v_{\text{SLIC}} = 28$ Hz, $\tau_{\text{SLIC}} = 177$
163 ms) match the theoretical conditions at high-field ($v_{\text{SLIC}} = 2J_{\text{intra}}$, $\tau_{\text{SLIC}} = 1/(\Delta J\sqrt{2})$). However, when the difference is small
164 ($\Delta\delta = 52$ Hz), the optimum SLIC conditions are $v_{\text{SLIC}} = 30.1$ Hz while $\tau_{\text{SLIC}} = 333$ ms. The change in v_{SLIC} is subtle (+ 7 %),
165 but the SLIC duration changes drastically (+ 83 %). Since aliphatic $-\text{CH}_2-$ groups in many of the selected molecules (Fig. 2)
166 have $\Delta\delta < 60$ Hz at 1.4 T, their SLIC duration τ_{SLIC} and SLIC amplitude v_{SLIC} must be re-optimised.



167 According to Fig. 5, the LLS yield after re-optimisation of v_{SLIC} and τ_{SLIC} , is 0.8 for
168 $\Delta\delta = 52$ Hz. We can compare it with the LLS yield in Fig. 4 (~ 0.35) to obtain the enhancement
169 factor. The ratio of the optimised LLS yield/non-optimised LLS yield is equal to: $0.8/0.35 \approx$
170 2.3.

171 Subsequently, we re-optimised τ_{SLIC} and v_{SLIC} for each molecule experimentally. The SLIC
172 conditions at 11.7 and 1.4 T are displayed in Table 1, whereas Table 2, shows the improvement
173 in the experimentally achieved LLS yield upon re-optimisation of τ_{SLIC} and v_{SLIC} at 1.4 T.

174 Table 1. Experimentally optimised SLIC conditions for 4-spin systems at low (1.4 T) and high (11.7 T) fields. The SLIC
175 amplitude v_{SLIC} changes for vitamin B1 and metronidazole, but remains unchanged for the other ligands. The duration τ_{SLIC}
176 increases at low magnetic field for ethanolamine, vitamin B1 and metronidazole.

Molecule	$\Delta\nu$ (Hz)	v_{SLIC} (Hz)	v_{SLIC} (Hz)	τ_{SLIC} (ms)	τ_{SLIC} (ms)
	at 1.4 T (60 MHz)	at 11.7 T (500 MHz)	at 1.4 T (60 MHz)	at 11.7 T (500 MHz)	at 1.4 T (60 MHz)
ethanolamine	54	25	25	190	340
lysine	80	27	27	205	205
vitamin B1	42	26	27	250	320
metronidazole	36	26	27	250	310
POEA	61	23	23	240	240

177

178 Table 2. LLS yield at 1.4 T before re-optimisation of v_{SLIC} and τ_{SLIC} (using the conditions listed in columns 3 and 5 in Table 1)
179 and after re-optimisation of v_{SLIC} and τ_{SLIC} (using the conditions listed in column 4 and 6 in Table 1). The LLS yield with
180 respect to the thermal signal (when the number of transients and the receiver gain remain the same) is lower than at
181 conventional high-field, where the yield is approximately $\sim 10\%$ (Sonnefeld et al., 2022a). However, the third column shows
182 that an enhancement, up to a factor of 3, has been achieved. This illustrates the need for re-optimisation of v_{SLIC} and τ_{SLIC} when
183 $\Delta\delta < 60$ Hz at low magnetic fields. For lysine and POEA for which the difference in chemical shifts $\Delta\delta > 60$ Hz, the SLIC
184 conditions were identical at 11.7 T and 1.4 T, so no increase in yield was observed.

Molecule	LLS Yield (with respect to thermal) (Non-optimised SLIC) / %	LLS Yield (with respect to thermal) (Optimised SLIC) / %	Enhancement Factor (Optimised/Non-opti- mised)
ethanolamine	0.68	2.06	3.0
lysine	1.89	1.89	1.0
vitamin B1	1.25	2.11	1.7
metronidazole	0.78	2.21	2.8
POEA	4.69	4.69	1.0

185

186

187

188



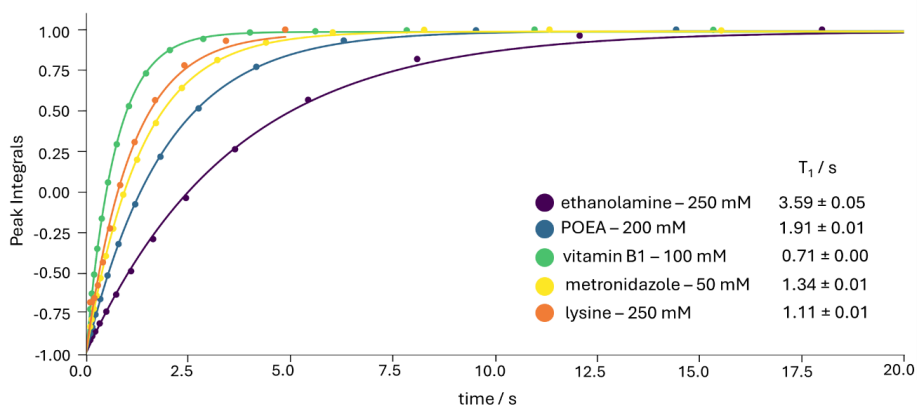
189 Comparing T_{LLS} and T_1 relaxation time constants at different magnetic fields

190 The T_1 and T_{LLS} of all five molecules shown in Fig. 2 were measured at low and high static
191 fields, in the same sample tubes, at the same concentrations, in the same solvents and at the
192 same temperatures. The concentrations were chosen to be high to warrant sufficient sensitivity
193 at low field, bearing in mind that the efficiency of two-way (“in-and-out”) SLIC is on the order
194 of only 10%. In the future we aim to enhance the sensitivity by combining SLIC at both low
195 and high fields with Dynamic Nuclear Polarisation [Vasos et al., 2009, Tayler et al., 2012,
196 Bornet et al., 2014, Kiryutin et al., 2019a, Kiryutin et al., 2019b, Razanahoera et al., 2024.]

197 The ratios of the relaxation rates of long-lived states ($R_{LLS} = 1/T_{LLS}$) and of longitudinal
198 magnetisation ($R_1 = 1/T_1$), are different at low and high fields (60 and 500 MHz for protons).
199 The ratio T_{LLS}/T_1 provides a measure of the usefulness of LLS for various applications such as
200 the measurement of slow motions [Sarkar et al., 2007], or small translation diffusion
201 coefficients [Cavadini et al., 2005].

202 Results and discussion

203 Inversion-recovery experiments at both low and high fields provided T_1 values for all samples.
204 The signal integrals of a chosen multiplet (see wavy arrows in Fig. 2) were plotted as a function
205 of the relaxation delay τ_{rel} . Fig. 6 shows the results obtained at low field. The same T_1
206 experiments were repeated at high magnetic field (11.7 T). The results are summarised in
207 Table 3.



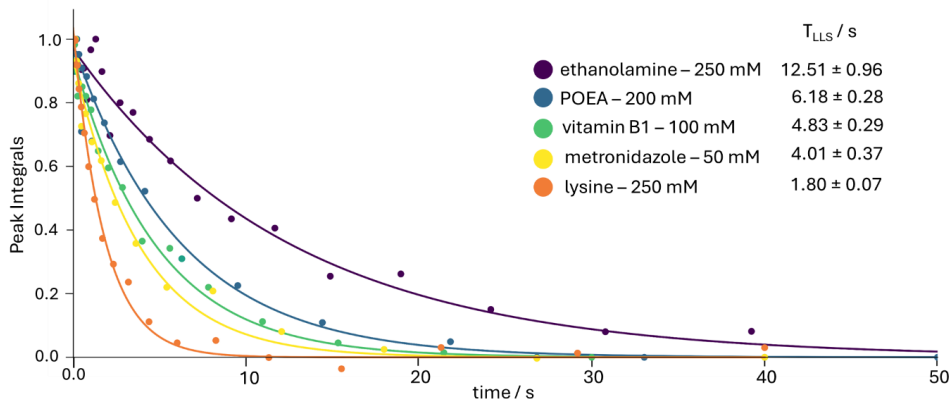
208

209 Figure 6. Longitudinal T_1 relaxation at low field (1.4 T) of the CH_2 protons highlighted by curly arrows in the 5 molecules
210 shown in Fig. 2, measured by inversion recovery.

211



212 To determine the lifetimes T_{LLS} at low field (1.4 T) by SLIC experiments, the delay τ_{rel} in
 213 Fig. 1 was incremented for each of the 5 molecules shown in Fig. 2.



214

215 Figure 7. LLS decays at low field (1.4 T) of the aliphatic CH₂ protons highlighted by curly arrows in the 5 molecules drawn
 216 Fig. 2.

217 Again, these experiments were also carried out with the same samples at high field. The high
 218 and low field results are shown in Tables 3 and 4. The effect of the magnetic field on the ratio
 219 T_{LLS}/T_1 is shown in Table 5.

220 Table 3. T_1 and T_{LLS} values at high field (11.7 T)

Molecule	Concentration (mM)	CH ₂ group (see Fig. 2)	T_1^{HF} /s (500 MHz)	T_{LLS}^{HF} /s (500 MHz)
ethanolamine	250	2	3.46 ± 0.01	10.33 ± 1.88
lysine	250	1	1.40 ± 0.01	4.33 ± 0.08
vitamin B1	100	2	0.73 ± 0.01	5.58 ± 0.27
metronidazole	50	2	1.27 ± 0.02	3.81 ± 0.14
POEA	200	1	2.21 ± 0.02	9.21 ± 0.49

221

222 Table 4. T_1 and T_{LLS} values at low field (1.4 T or 60 MHz for protons)

Molecule	Concentration (mM)	CH ₂ group (see Fig. 2)	T_1^{LF} /s (60 MHz)	T_{LLS}^{LF} /s (60 MHz)
ethanolamine	250	2	3.59 ± 0.05	12.51 ± 0.96
lysine	250	1	1.11 ± 0.01	1.80 ± 0.07
vitamin B1	100	2	0.71 ± 0.00	4.83 ± 0.29
metronidazole	50	2	1.34 ± 0.01	4.01 ± 0.37
POEA	200	1	1.91 ± 0.01	6.18 ± 0.28

223

224

225



226 Table 5. Ratios T_{LLS}/T_1 at high field (11.7 T) and at low field (1.4 T).

Molecule in D ₂ O	Concentration (mM)	enhancement $(T_{LLS}/T_1)^{HF}$ (500 MHz)	enhancement $(T_{LLS}/T_1)^{LF}$ (60 MHz)	ratio of enhancements HF/LF
ethanolamine	250	3.0	3.5	0.86
lysine	250	3.1	1.6	1.94
vitamin B1	100	7.6	6.8	1.12
metronidazole	50	3.0	3.0	1.00
POEA	200	4.2	3.2	1.31

227

228 Comparison between the relaxation times T_{LLS} and T_1 at high field gives a range $3.0 < T_{LLS}/T_1$
229 < 4.2 for all molecules except vitamin B1, which has an exceptional gain $T_{LLS}/T_1 = 7.6$. At low
230 field, by contrast, the ratios lie in the range of $3.0 < T_{LLS}/T_1 < 6.8$ for all molecules except
231 lysine, which has a rather modest gain $T_{LLS}/T_1 = 1.6$. In summary, the T_{LLS}/T_1 ratios at high
232 field (11.7 T) are either slightly higher or similar as at low field (1.4 T), except for ethanolamine
233 where the enhancement is 17 % higher at low field.

234

Conclusions

235 The yield of the excitation of LLS by SLIC at low fields depends on the chemical shift
236 difference $\Delta\delta$ between the neighbouring spin pairs. When $\Delta\delta \leq 60$ Hz, the pulse amplitude,
237 v_{SLIC} , and duration, τ_{SLIC} , must be optimised experimentally starting at the high-field
238 conditions. The T_{LLS}/T_1 ratios at low field (1.4 T) are either slightly lower or similar as at high
239 field.

Data availability

241 The Spin Dynamica codes used to calculate Figures 4 and 5 are available through the Zenodo
242 repository under [10.5281/zenodo.18684154](https://zenodo.org/record/18684154)

Author Contributions

244 K.S. designed the research. S.V.D. and C.W. performed the experiments and analysed the data. All
245 authors contributed to writing the paper.

Conflict of Interest

247 G.B. is a member of the editorial board of Magnetic Resonance of the Groupement Ampere. The
248 authors have no other competing interests to declare.

Financial Support

250 This work was supported by the European Research Council (ERC), Synergy grant “Highly
251 Informative Drug Screening by Overcoming NMR Restrictions” (HISCORE, grant agreement number
252 951459). K.S. acknowledges support by l’Agence Nationale de la Recherche (ANR) on the project
253 THROUGH-NMR (ANR-24-CE93-0011-01).



254 References

- 255 Bengs, C., & Levitt, M. H. (2018). SpinDynamica: Symbolic and numerical magnetic resonance in a
256 Mathematica environment. *Magnetic Resonance in Chemistry*, 56(6), 374–414.
257 <https://doi.org/10.1002/mrc.4642>
- 258 Bornet, A., Ji, X., Mammoli, D., Vuichoud, B., Milani, J., Bodenhausen, G., and Jannin, S.: Long-
259 Lived States of Magnetically Equivalent Spins Populated by Dissolution-DNP and Revealed by
260 Enzymatic Reactions, *Chem. – Eur. J.*, 20, 17113–17118, <https://doi.org/10.1002/chem.201404967>,
261 2014.
- 262 Carravetta, M., & Levitt, M. H. (2004). Long-lived nuclear spin states in high-field solution NMR.
263 *Journal of the American Chemical Society*, 126(20), 6228–6229. <https://doi.org/10.1021/ja0490931>
- 264 Cavadini, S., Dittmer, J., Antonijevec, S., and Bodenhausen, G.: Slow Diffusion by Singlet State NMR
265 Spectroscopy, *J. Am. Chem. Soc.*, 127, 15744–15748, <https://doi.org/10.1021/ja052897b>, 2005.
- 266 DeVience, S. J., Walsworth, R. L., and Rosen, M. S.: Preparation of Nuclear Spin Singlet States Using
267 Spin-Lock Induced Crossing, *Phys. Rev. Lett.*, 111, 173002,
268 <https://doi.org/10.1103/PhysRevLett.111.173002>, 2013.
- 269 Kiryutin, A. S., Panov, M. S., Yurkovskaya, A. V., Ivanov, K. L., and Bodenhausen, G.: Proton
270 Relaxometry of Long-Lived Spin Order, *ChemPhysChem*, 20, 766–772,
271 <https://doi.org/10.1002/cphc.201800960>, 2019a.
- 272 Kiryutin, A. S., Pravdivtsev, A. N., Yurkovskaya, A. v., Vieth, H.-M., & Ivanov, K. L.: Nuclear Spin
273 Singlet Order Selection by Adiabatically Ramped RF Fields. *The Journal of Physical Chemistry B*,
274 120(46), 11978–11986. <https://doi.org/10.1021/acs.jpcc.6b08879>, 2016.
- 275 Kiryutin, A. S., Rodin, B. A., Yurkovskaya, A. V., Ivanov, K. L., Kurzbach, D., Jannin, S., Guarin, D.,
276 Abergel, D., and Bodenhausen, G.: Transport of hyperpolarized samples in dissolution-DNP
277 experiments, *Phys. Chem. Chem. Phys.*, 21, 13696–13705, <https://doi.org/10.1039/C9CP02600B>,
278 2019b.
- 279 Razanaoera, A., Sonnefeld, A., Sheberstov, K., Narwal, P., Minaei, M., Kouřil, K., Bodenhausen, G.,
280 and Meier, B.: Hyperpolarization of Long-Lived States of Protons in Aliphatic Chains by Bullet
281 Dynamic Nuclear Polarization, Revealed on the Fly by Spin-Lock-Induced Crossing, *J. Phys. Chem.*
282 *Lett.*, 15, 9024–9029, <https://doi.org/10.1021/acs.jpcclett.4c01457>, 2024.
- 283 Sabba, M., Wili, N., Bengs, C., Whipham, J. W., Brown, L. J., and Levitt, M. H.: Symmetry-based
284 singlet–triplet excitation in solution nuclear magnetic resonance, *J. Chem. Phys.*, 157, 134302,
285 <https://doi.org/10.1063/5.0103122>, 2022.
- 286 Sarkar, R., Vasos, P. R., and Bodenhausen, G.: Singlet-State Exchange NMR Spectroscopy for the
287 Study of Very Slow Dynamic Processes, *J. Am. Chem. Soc.*, 129, 328–334,
288 <https://doi.org/10.1021/ja0647396>, 2007.
- 289 Sheberstov, K. F., Kiryutin, A. S., Bengs, C., Hill-Cousins, J. T., Brown, L. J., Brown, R. C. D., Pileio,
290 G., Levitt, M. H., Yurkovskaya, A. V., and Ivanov, K. L.: Excitation of singlet–triplet coherences in
291 pairs of nearly-equivalent spins, *Phys. Chem. Chem. Phys.*, 21, 6087–6100,
292 <https://doi.org/10.1039/C9CP00451C>, 2019a.
- 293 Sonnefeld, A., Razanaoera, A., Pelupessy, P., Bodenhausen, G., and Sheberstov, K.: Long-lived
294 states of methylene protons in achiral molecules, *Sci. Adv.*, 8, eade2113,
295 <https://doi.org/10.1126/sciadv.ade2113>, 2022a.



- 296 Sonnefeld, A., Bodenhausen, G., and Sheberstov, K.: Polychromatic Excitation of Delocalized Long-
297 Lived Proton Spin States in Aliphatic Chains, *Phys. Rev. Lett.*, 129, 183203,
298 <https://doi.org/10.1103/PhysRevLett.129.183203>, 2022b.
- 299 Stevanato, G., Hill-Cousins, J. T., Håkansson, P., Roy, S. S., Brown, L. J., Brown, R. C. D., Pileio, G.,
300 and Levitt, M. H.: A Nuclear Singlet Lifetime of More than One Hour in Room-Temperature Solution,
301 *Angew. Chem. Int. Ed.*, 54, 3740–3743, <https://doi.org/10.1002/anie.201411978>, 2015.
- 302 Tayler, M. C. D.: Filters for Long-lived Spin Order, <https://doi.org/10.1039/9781788019972-00188>,
303 2020.
- 304 Tayler, M. C. D., Marco-Rius, I., Kettunen, M. I., Brindle, K. M., Levitt, M. H., and Pileio, G.: Direct
305 Enhancement of Nuclear Singlet Order by Dynamic Nuclear Polarization, *J. Am. Chem. Soc.*, 134,
306 7668–7671, <https://doi.org/10.1021/ja302814e>, 2012.
- 307 Vasos, P. R., Comment, A., Sarkar, R., Ahuja, P., Jannin, S., Ansermet, J.-P., Konter, J. A., Hautle, P.,
308 van den Brandt, B., and Bodenhausen, G.: Long-lived states to sustain hyperpolarized magnetization,
309 *Proc. Natl. Acad. Sci.*, 106, 18469–18473, <https://doi.org/10.1073/pnas.0908123106>, 2009.